

DIAGNOSTICS

Detection of pathological biomarkers in human clinical samples via amplifying genetic switches and logic gates

Alexis Courbet,¹ Drew Endy,² Eric Renard,³ Franck Molina,^{1*} Jérôme Bonnet^{4*}

Whole-cell biosensors have several advantages for the detection of biological substances and have proven to be useful analytical tools. However, several hurdles have limited whole-cell biosensor application in the clinic, primarily their unreliable operation in complex media and low signal-to-noise ratio. We report that bacterial biosensors with genetically encoded digital amplifying genetic switches can detect clinically relevant biomarkers in human urine and serum. These biosensors perform signal digitization and amplification, multiplexed signal processing with the use of Boolean logic gates, and data storage. In addition, we provide a framework with which to quantify whole-cell biosensor robustness in clinical samples together with a method for easily reprogramming the sensor module for distinct medical detection agendas. Last, we demonstrate that biosensors can be used to detect pathological glycosuria in urine from diabetic patients. These next-generation whole-cell biosensors with improved computing and amplification capacity could meet clinical requirements and should enable new approaches for medical diagnosis.

INTRODUCTION

In vitro diagnostic tests (IVDs) are growing in importance in the global health arena because of their noninvasive nature and resulting ease of use and scale (1, 2). However, conventional detection methods for IVDs are often expensive and complex, and thus difficult to implement in resource-limited settings (3). In response to these challenges, bioengineers have developed attractive methodologies that rely on synthetic nanoprobe (4–6) or microfluidics (7, 8). Yet, there remains a need for easy-to-use, portable biosensor devices that can be used by nonspecialists to make clinical measurements at home or in remote locations (4, 9, 10).

Among biosensing devices, whole-cell biosensors mainly based on bacteria have proven to be applicable for the detection and quantification of a wide range of analytes (11, 12). Living cells have many attractive properties when it comes to diagnostics development. Cells detect biomolecules with high sensitivity and specificity and are capable of integrated and complex signal processing. Cells also provide a self-manufacturing platform via autonomous replication (12, 13), and the production of laboratory prototypes can be scaled using existing industrial frameworks (14). Spores from whole-cell biosensors can remain functional for extended periods of time, increasing the shelf life of a diagnostic product in harsh storage conditions (15). Last, whole-cell biosensors are highly versatile and can be used as stand-alone devices or interfaced with other technologies such as electronics, microfluidics, or micropatterning (16–18). All of these advantages have prompted the development of whole-cell biosensors that measure a variety of clinical parameters (19–24). However, whole-cell biosensor systems have not yet been applied for the monitoring of medically relevant parameters in a clinical context.

Many challenges have limited whole-cell biosensor translation to the clinic: (i) unreliable operation and low signal-to-noise ratio in complex and heterogeneous clinical samples; (ii) the inability to engi-

neer ligand-tailored sensors; (iii) limited signal-processing capability, which precludes the integration of several biomarker signals for accurate diagnosis; (iv) lack of consistent frameworks for the assessment of robustness in challenging clinical conditions; (v) response times that are not compatible for diagnosis that require fast delivery of results; and (vi) compliance to clinical formats (fig. S1).

The emerging field of synthetic-biology research aims at streamlining the rational engineering of biological systems (25). In the field of health care, synthetic biology has delivered breakthroughs in drug biosynthesis (26–29) and new hope for compelling translational medicine applications (30–32). As proof of concept, researchers have embedded medical algorithms within living cells for diagnosis, disease classification, and treatment (33–37). However, the use of synthetic biology tools and concepts to improve IVD technologies has been limited mainly to bacteriological tests using engineered bacteriophages (38) or to a recently developed mammalian cell-based allergy profiler (39).

Synthetic biology focuses on parts and systems standardization, the engineering of modular components, and systematic strategies for the engineering of biological systems and new biological functions with reliable and predictable behaviors. Molecular modules such as sensors, reporters, or switches could ultimately be assembled at a systems level to perform specific tasks. Genetic devices that support in vivo computation were developed recently and enable living cells to perform sophisticated signal-processing operations such as Boolean logic, edge detection, or cellular profiling (40, 41). Therefore, synthetic biology could presumably support the design of cell-based biosensors that meet medical specifications and help to translate whole-cell biosensors to clinical applications.

Here, we investigate the use of recently developed digital amplifying genetic switches and logic gates (42) to bring the performance of whole-cell biosensor closer to clinical requirements. These genetic devices enabled bacteria to perform, in human clinical samples, reliable detection of clinically relevant biomarkers, multiplexing logic, and data storage. We also provide a framework for quantifying whole-cell biosensor robustness in clinical samples together with a method for easy reprogramming of the sensor module for distinct medical detection agendas. Hence, our platform architecture is highly modular and could be repurposed for various applications. We anticipate that such

¹Sys2Diag FRE3690-CNRS/ALCEDIAG, Cap Delta, 34090 Montpellier, France. ²Department of Bioengineering, Stanford University, Stanford, CA 94305, USA. ³Department of Endocrinology, Diabetes, Nutrition, Montpellier University Hospital; INSERM 1411 Clinical Investigation Center; Institute of Functional Genomics, CNRS UMR 5203, INSERM U661, University of Montpellier, 34090 Montpellier, France. ⁴Centre de Biochimie Structurale, INSERM U1054, CNRS UMR5048, University of Montpellier, 29 Rue de Navacelles, 34090 Montpellier, France.

*Corresponding author. E-mail: jerome.bonnet@inserm.fr (J.B.); franck.molina@sys2diag.cnrs.fr (F.M.)

engineered bacterial biosensors (“bactosensors”) that are capable of in vivo computation could be tailored according to medical knowledge and used as expert biosensing devices for medical diagnosis (Fig. 1 and fig. S1).

RESULTS

Behavior and robustness of bacterial chassis in human clinical samples

Our first goal was to determine the operational characteristics of bacterial chassis of interest in terms of growth, viability, and functionality of gene networks in human body fluids of clinical relevance: urine and blood serum. We chose to evaluate the robustness of Gram-negative and Gram-positive bacterial models—*Escherichia coli* and *Bacillus subtilis*, respectively—that have been used in previous whole-cell biosensors designs. To this end, we collected urine and serum from healthy volunteers, pooled the samples to average molecule concentrations to account for possible variations among individuals, and prepared dilutions with a defined culture medium (see Materials and Methods). We then inoculated various clinical sample dilutions with cells from stationary cultures of *E. coli* DH5 α Z1 or *B. subtilis* 168, grew these cultures for 18 hours at 25°, 30°, or 37°C, and measured their optical densities. For both cell types, we observed cell growth across the complete range of sample dilutions and at all three temperatures

(fig. S2). However, growth was strongly inhibited at 100% urine or serum concentrations, probably because of the lack of nutrient provided by the diluted culture medium. Growth of both cell types decreased with increasing urine or serum concentration, but cell death was insignificant (<2% for all samples; fig. S3). These results demonstrate that both Gram-positive and Gram-negative bacteria can survive and proliferate in human clinical samples for several hours. Because of the larger number of tools available for the reliable control of gene expression (43, 44), we chose *E. coli* for further engineering of a prototype bactosensor.

We next assessed the capacity of *E. coli* cells growing in clinical samples to respond in a reliable way to exogenously added molecular signals using the model transcriptional promoters pTET [which responded to anhydrotetracycline (aTc)] and pBAD [which responded to arabinose (ara)], both driving expression of a reporter gene that encodes the green fluorescent protein (GFP). Both promoters were functional at all concentrations of clinical samples (Fig. 2, A and B), but cells that were induced in 100% serum failed to produce GFP, which indicates that serum has an inhibitory effect on bacterial gene expression. Increasing sample concentrations produced variations in auto-fluorescence, which could be corrected using a reference promoter (45). Such reference promoters could be used as internal standards to increase measurement reliability in a clinical setting (fig. S4 and note S1). These results demonstrate that synthetic gene networks can remain functional in clinical samples.

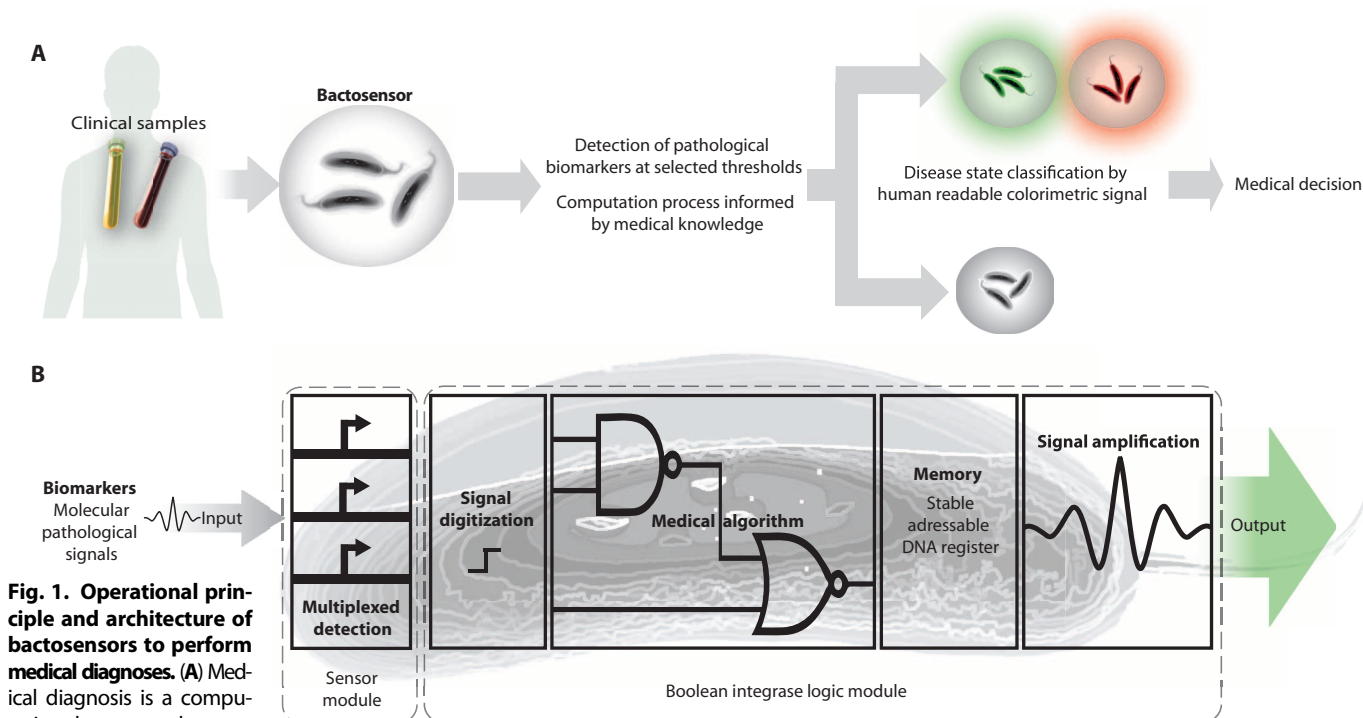


Fig. 1. Operational principle and architecture of bactosensors to perform medical diagnoses. (A) Medical diagnosis is a computational process that can be formalized using Boolean logic in vivo and embedded into a bactosensor. The bactosensor is capable of detecting a pattern of specific biomarkers in human clinical samples at selected thresholds and integrates these signals using an in vivo computational process. If a pathological pattern of biomarker is detected, the bactosensor generates a colorimetric output. (B) Schematic architecture of a bactosensor. A sensor module enables multiplexed detection

of pathological biomarkers. These control signals drive a Boolean integrase logic gate module, which is the biological support for a user-defined digital medical algorithm. Boolean integrase logic gates also enable signal digitization and amplification along with storage of the diagnosis test’s outcome in a stable DNA register that can be interrogated a posteriori.

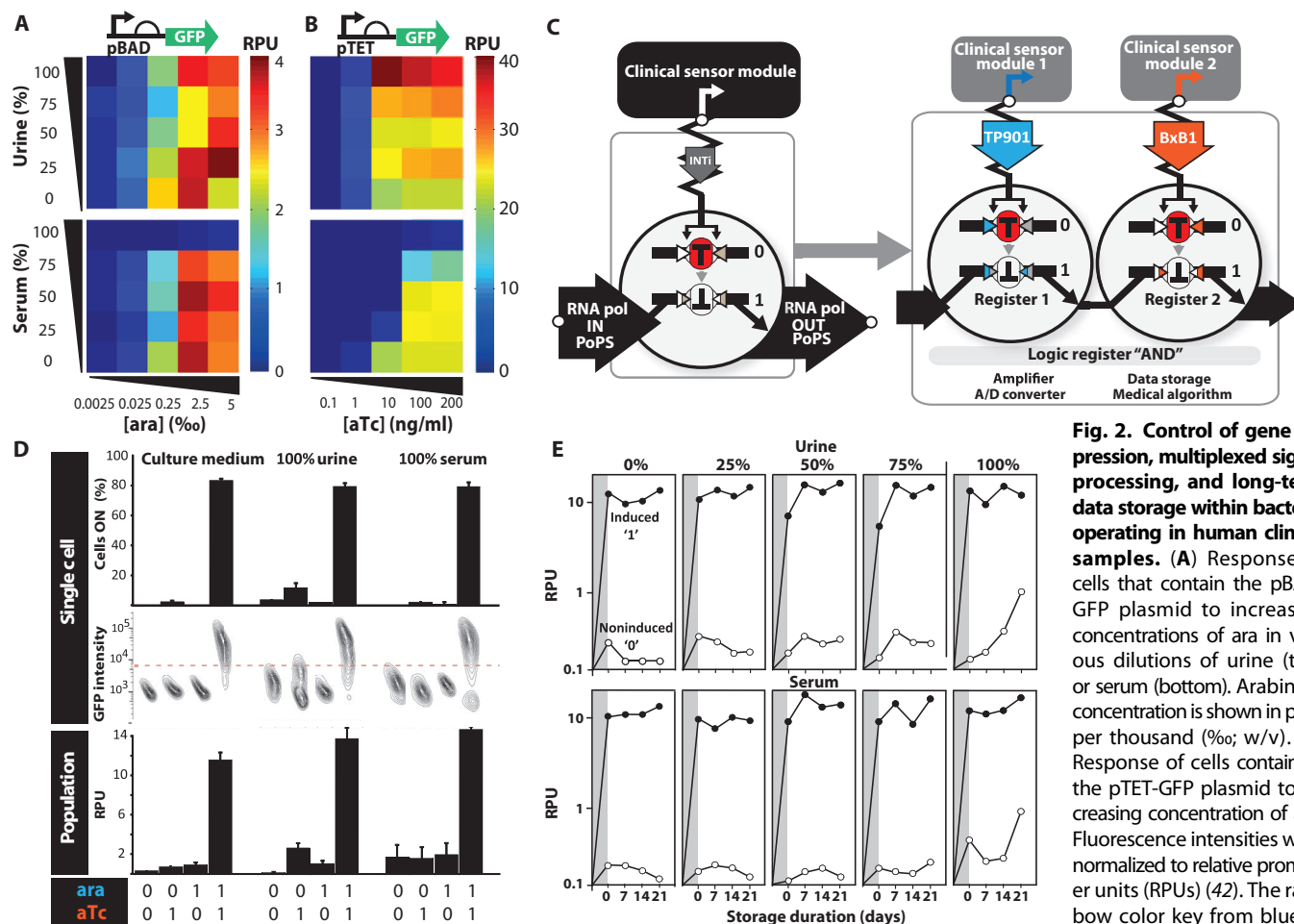


Fig. 2. Control of gene expression, multiplexed signal processing, and long-term data storage within bacteria operating in human clinical samples. (A) Response of cells that contain the pBAD-GFP plasmid to increasing concentrations of ara in various dilutions of urine (top) or serum (bottom). Arabinose concentration is shown in parts per thousand (‰; w/v). **(B)** Response of cells containing the pTET-GFP plasmid to increasing concentration of aTc. Fluorescence intensities were normalized to relative promoter units (RPU) (42). The rainbow color key from blue to red depicts increasing signal

intensities measured in RPU. **(C)** Architecture and functional composition of transcriptor-based digital amplifying genetic switches. The clinical sensor promoter drives integrase expression, which inverts a transcriptor module that controls the flow of RNA polymerase (RNA pol) along the DNA. Two transcriptors that respond to different signals can be composed in a series to produce an AND gate. A/D, analog to digital. **(D)** Operation of an AND gate at 25°C, at various dilutions (0, 100%) of human urine and serum in response to ara (0.5% w/v) and aTc (200 ng/ml). The 0 or 1 values symbolize absence or presence, respectively, of a particular inducer. Population (bottom, RPU) and single-cell (top) fluorescence intensity measurements are shown. The middle row shows raw flow cytometry data (x axis: side scatter). Errors bars indicate SDs from three independent experiments, each performed in triplicate. **(E)** Stability of functional memory in various dilutions of urine (top row) or serum (bottom row) in living cells. The AND gate was switched with 0.5% (w/v) ara and aTc (200 ng/ml). Cells were then kept at 4°C for 7, 14, or 21 days and then grown overnight in fresh medium. For each medium concentration, GFP fluorescence in RPU is represented for non-induced cells (open circles) and induced cells (filled circles). The gray-shaded regions depict the duration of the period in which cells were exposed to the inducing signal.

Multiplexing logic and memory in human clinical samples

Multiplexed biomarker assays are known to improve the performance and robustness of diagnostic tests (3). Signal processing allows an assay to integrate the detection of multiple inputs and to perform complex analytical tasks such as diagnostics algorithms informed by medical knowledge. Performing such integrated multiplexed detection and analysis within living cells thus requires some form of engineered biomolecular computation. We recently designed three-terminal devices, termed transcriptors, that use serine integrase enzymes to control the flow of RNA polymerase along DNA via unidirectional inversion of an asymmetric transcriptional terminator (42, 46).

Transcriptors are digital amplifying switches that operate as analog-to-digital converters, are capable of signal amplification, can perform data storage and record transient signals, and can be composed to pro-

duce a variety of Boolean integrase logic gates (Fig. 2C). We thus wanted to assess whether Boolean integrase logic gates could enable whole-cell biosensors, operating in clinical samples, to execute complex signal-processing algorithms. To improve the performance of synthetic circuits for the clinics, we incorporated in our design recently developed standardized regulatory genetic elements (see note S2). We first evaluated the functionality and robustness of an AND gate that responded to ara and aTc in clinical samples and found that the logic gate operated reliably at room temperature in 100% urine and serum (Fig. 2D). We obtained similar results using NAND and NOR gates (fig. S5). Moreover, after gate switching, cells stored at 4°C could be regrown and the fluorescent output measured after up to 3 weeks of storage time (Fig. 2E). Moreover, the signal stored within the DNA register could be recovered from bacterial cells that had been dead for

8 months using the polymerase chain reaction (PCR) or Sanger DNA sequencing (fig. S6). Together, these results show that living cells with embedded Boolean integrase logic gates can perform programmable, multiplexed signal processing in clinical samples. The ability to perform stable data storage over extended periods of times provides new opportunities for delayed readout in clinical environments.

Analytical evaluation of biosensors for the detection of biological parameters in clinical samples

We next aimed to detect signals of clinical interest in urine and serum. We first chose nitrogen oxides (NO_x), a biomarker for various pathologies involving inflammation (47). Using a GFP reporter, we measured the response of pYeaR, a nitrite/nitrate-sensitive transcriptional promoter (48), to increasing concentrations of NO_x at various urine and serum dilutions (Fig. 3A). The pYeaR activation threshold decreased with increasing concentrations of urine or serum and was activated in 100% urine without the addition of NO_x, probably due to the presence of endogenous NO_x. Moreover, pYeaR was totally inhibited in 100% serum. These results highlight the sensitivity of whole-cell biosensors to context perturbations that need to be overcome for successful medical applications.

Thresholding, digitization, and amplification of biologically relevant signals in clinical samples using digital amplifying genetic switches

We then tested whether transcription-based digital amplifying switches could improve the detection of signals of clinical interest. We thus cloned pYeaR upstream of the *Bxb1* or *TP901-1* integrase genes, which encode the enzymes that control transcription switching. Because even weak, leaky promoter activity can drive integrase expression and non-specific switching, we used a directed evolution approach that combined randomization of regions that regulate integrase gene expression [that is, the ribosomal binding site (RBS), ATG translation start codon, and nucleic acid sequences that encode a C-terminal SsrA tag for cytoplasmic degradation] coupled with bacterial library screening to obtain switches that activated in response to NO_x (Fig. 3B). From this library, we selected and characterized three switches that contained variations in the RBS, start codon, integrase type, and SsrA proteolysis tag (46, 49). Switches were activated at different NO_x thresholds that spanned several orders of magnitude (Fig. 3C). These data suggest that digital amplifying genetic switches could be tailored to detect a specific biomarker over defined pathological thresholds that meet clinical requirements (fig. S7).

We then mapped the transfer function of one of the switches at various sample dilutions (Fig. 3D) and observed signal digitization and marked improvement of the signal-to-noise ratio compared to the pYeaR-GFP construct. The inhibitory effect of 100% serum on NO_x detection was overcome, although signal interference was still observed in 100% urine. Using an amplification reporter system, we quantified pYeaR switch-mediated signal amplification across a range of signals and sample concentrations (Fig. 3E) and measured maximum gain values between 10 and 15 dB (decibels). These results show that digital amplifying switches increase the robustness of whole-cell biosensing systems and could thus enable the development of clinically compliant biosensors.

Detection of a metabolized biological signal—glucose—in clinical samples

Glucose is a biomarker of clinical interest whose blood levels can be used for the monitoring of diabetes (high blood glucose or glycemia)

and whose presence in urine (glycosuria) marks the onset of or presence of uncontrolled diabetes. Point-of-care technologies that enable clinicians to detect glycosuria or continuously monitor glycemia remotely can greatly improve and simplify care of diabetic patients (50). The fact that glucose is one of the primary carbon sources metabolized by bacterial cells makes it a challenging molecular signal to monitor. To perform glucose detection, we chose the pCpxP promoter as a driver of target gene expression, which is activated in the presence of glucose, pyruvate, or acetate (51). pCpxP showed a high basal level of expression in bacterial growth medium and human serum and a low signal-to-noise ratio (Fig. 4A, maximum fold change ~1.5 in medium, ~2.2 in urine, and ~1.7 in serum). Moreover, pCpxP was inhibited by increasing urine concentrations and glucose concentration greater than 10⁻² M. For the latter case, we confirmed, by kinetic assays, the time-dependent inhibition of pCpxP putatively as a result of a glucose-induced drop in the pH of the medium (52) (fig. S8).

We next built a pCpxP switch and again observed a marked improvement in the signal-to-noise ratio (Fig. 4A, maximum fold changes ~12.4 in medium, 12.6 in urine, and ~20.6 in serum) and a near-digital switching (that is, the system responded in a nearly all-or-none fashion). Response of the pCpxP switch to glucose was detectable up to 100% urines, indicating that a low signal produced by the promoter in these conditions was detected, amplified, and stored by the switch. The transient pCpxP activity at high glucose concentrations was also detected and stored by the pCpxP switch (Fig. 4A and fig. S8). Therefore, the detection of multiple clinically relevant signals can be systematically improved by digital amplifying switches. Finally, as a proof of concept, we performed dual detection and multiplexed signal processing of clinical biomarkers by building two-input logic gates controlled by NO_x and glucose and performing various computation processes (fig. S9).

Quantifying biosensor robustness in clinical samples

We next quantified the improvement in signal digitization conferred by the digital amplifying switches. For both pYeaR and pCpxP, we measured the digitization error rates (DERs; the combined probability of scoring a false-positive or a false-negative) (42) of promoter-only constructs and promoter-switch constructs in the presence of minimal and maximal inducer concentrations (fig. S10). We found that sensors that incorporated digital amplifying switches generally displayed a reduced DER, demonstrating the improvement in signal digitization provided by the switches.

We then aimed at establishing a quantitative framework with which to evaluate the robustness of the biosensor response against clinical sample-induced perturbations (fig. S11). At each inducer concentration and for each clinical sample dilution, we quantified the change in signal relative to cells grown in culture medium. The relative changes in signal values were averaged to obtain a global robustness score (RS), which was inversely proportional to the robustness of the biosensor against sample-induced perturbations. For pCpxP, use of the switch reduced RS values from 0.6 to 0.3 in urine and from 0.27 to 0.20 in serum. For pYeaR, RS values decreased from 2.1 to 0.44 in urine and from 1.15 to 0.69 in serum. Using digital amplifying switches thus systematically improved the robustness of the biosensor response against sample perturbations. Part of this improvement in robustness also resulted from the use of standard parts for the translational control of the switch output (43) (fig. S12 and note S2).

Together, these results demonstrate that digital amplifying switches can markedly improve the reliability of the detection of clinically relevant signals in clinical samples.

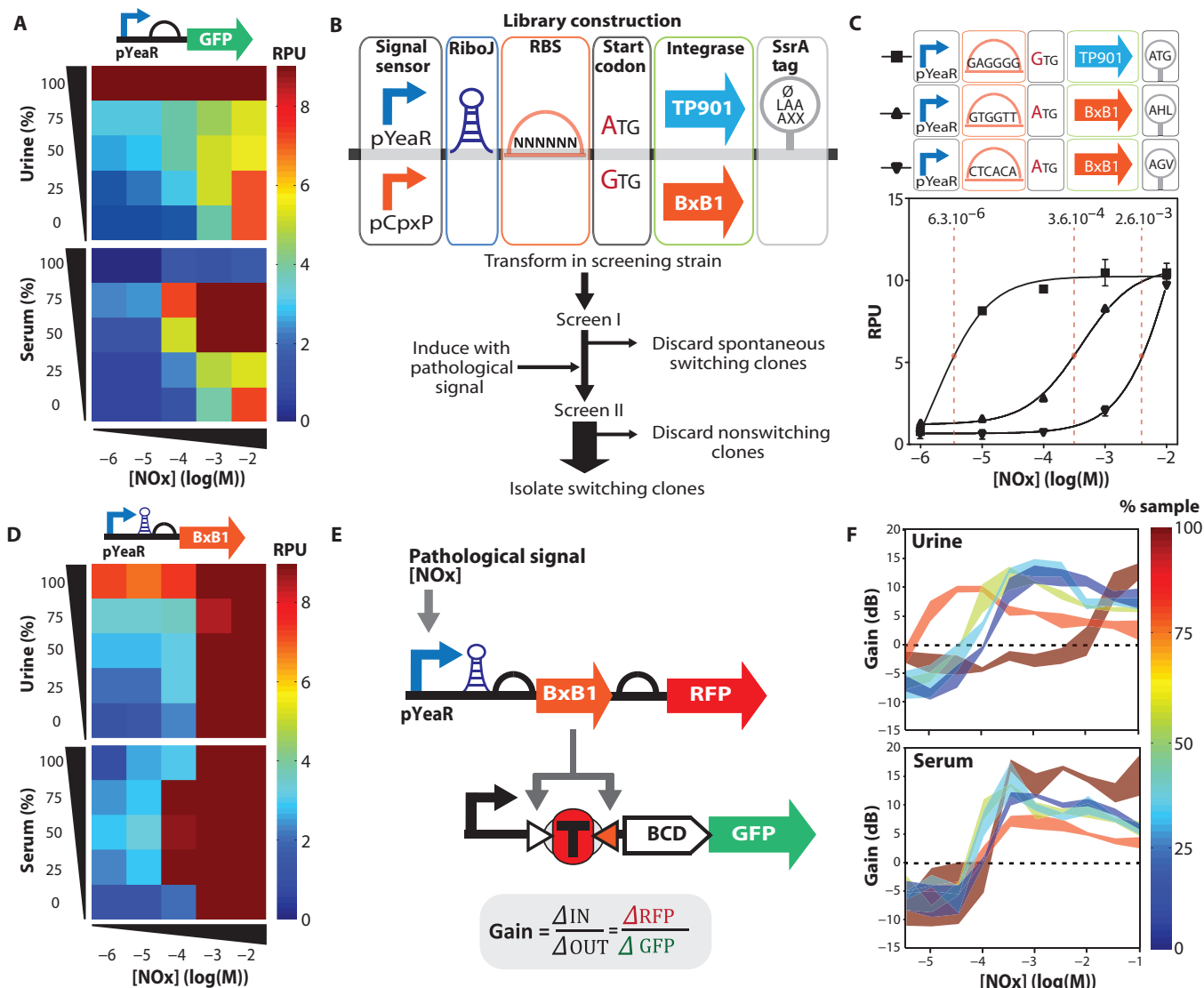


Fig. 3. Thresholding, digitization, and amplification of biologically relevant signals in clinical samples using amplifying genetic switches.

(A) Characterization of the NO_x-responsive promoter pYeaR driving expression of GFP in various dilutions of serum and urine. The rainbow color key from blue to red depicts increasing signal intensities measured in RPU. (B) Workflow for connecting biological signal-responding promoters to amplifying digital switches. An integrase expression cassette library driven by promoters of interest was built by introducing combinatorial diversity in RBSs, start codons, and C-terminal SsrA degradation tags. Libraries were transformed in a screening strain, spontaneously switching clones were eliminated, and the remaining cells were induced with the biological signal of interest. Switching clones were identified on a plate reader or using a fluorescence-activated cell sorter and isolated (see Materials and Methods for details). (C) Multiple switching threshold for biomarker detection. Clones were isolated from the various pYeaR li-

braries and characterized. Midpoint switching values are indicated. Variation in sequences among the isolated clones is depicted in the upper panel, along with the correspondence between graphs symbols and a particular switch sequence. (D) Digitization and amplification of the NO_x signal in urine and serum using amplifying digital switches. Cells cotransformed with pYeaR switch and exclusive OR (XOR)-GFP gates (42) were induced with NO_x, and bulk fluorescence was measured on a plate reader. (E) The plasmid to measure amplification of NO_x input consists of bicistronic BxB1-RFP cassette driven by pYeaR. This construct was cotransformed with a XOR-GFP gate to enable the precise simultaneous measurement of fold change in input control signal (RFP) and output signal (GFP) after induction with NO_x. (F) In vivo molecular pathological signal amplification in clinical samples. Gain in decibels was calculated as the 10log of the RFP/GFP ratio. The line thickness represents the SD over three independent experiments.

Bactosensor detection of glycosuria in clinical samples from diabetic patients

To assess the relevance of digital amplifying switches for disease detection in a clinical assay, we sought to develop a proof-of-concept sensor that detects endogenous levels of a pathological biomarker

in clinical samples from patients. As a preliminary validation and proof of concept, we aimed to detect glycosuria using the pCpxP switch.

To do so, we used a prototype clinical format and encapsulated viable bactosensors in polyvinyl acetate (PVA)/alginate hydrogel beads

Downloaded from stm.sciencemag.org on May 28, 2015

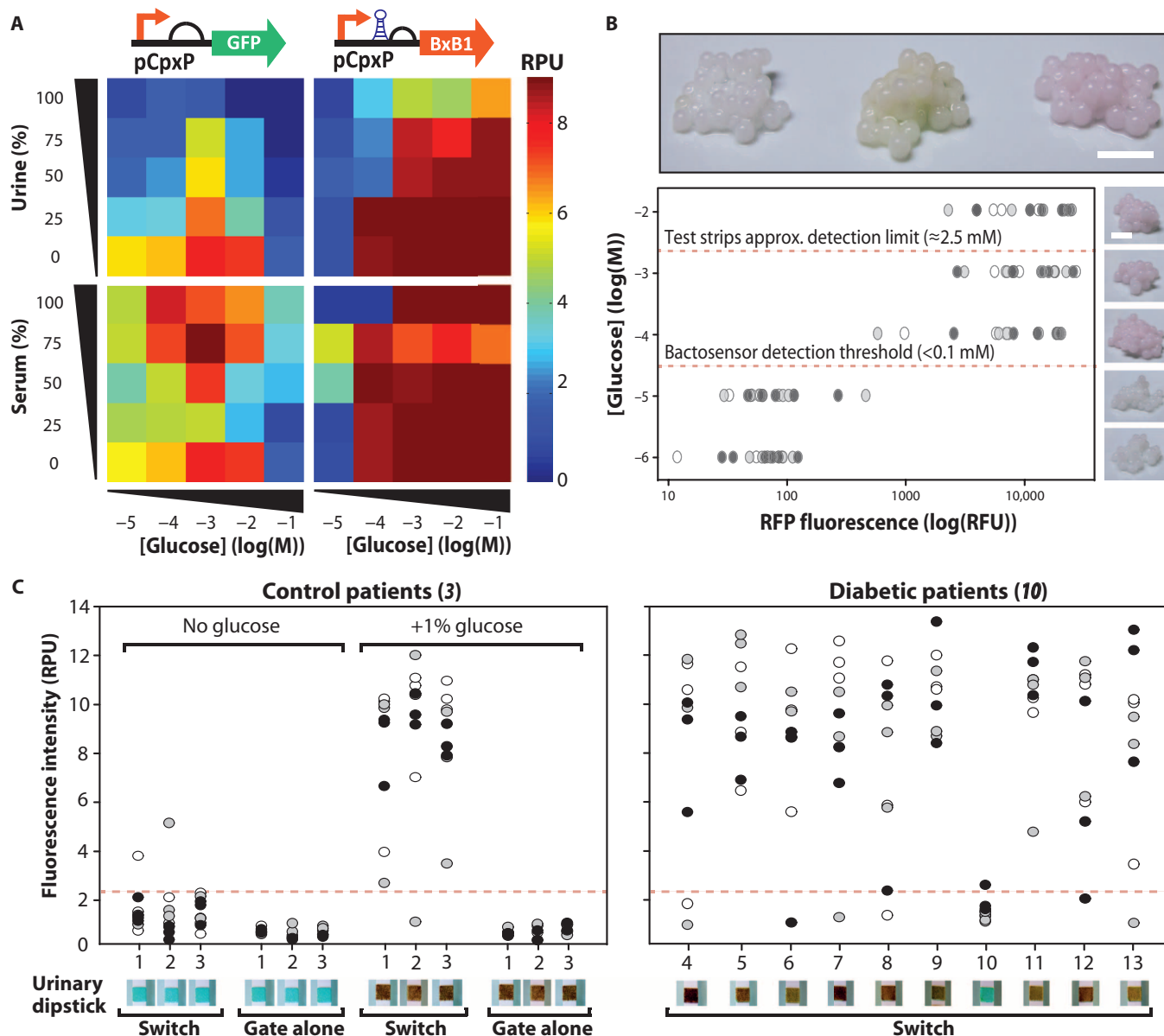


Fig. 4. Bactosensor-mediated detection of pathological glucose levels in clinical samples from diabetic patients. (A) Comparison of the response of pCpxP-GFP (left) and pCpxP-Bxb1 (right) constructs to increasing concentrations of glucose in various concentrations of urine (upper panel) or serum (lower panel). (B) Upper panel: Insulation of bactosensors in stable hydrogel beads. Left: Uninduced beads. Middle: NOx-induced beads with GFP reporter. Right: NOx-induced beads with RFP reporter. Scale bar, 0.5 cm. Lower panel: Operability of amplifying digital switches encapsulated in PVA/alginate beads. Beads that contained cells cotransformed with the XOR-RFP gate and pCpxP-TP901 were incubated in culture medium supplemented with various inducer concentrations, and RFP fluorescence was measured after 24 hours. RFU, relative fluorescence unit. Detection thresholds for urinary dipsticks and for bactosensor are indicated. Pictures of the beads at various inducer concentrations are shown. Scale bar, 0.5 cm. (C) Bactosensor-

mediated detection of abnormal glycosuria levels in clinical samples from diabetic patients. PVA/alginate beads encapsulating cells transformed with both the pCpxP-TP901 controller and the XOR-GFP gate, XOR-GFP gate alone, or the reference construct J23100-GFP were incubated in urine samples. Left panel: three glucose-negative samples from independent individuals and three positive controls [same samples supplemented with 1% (w/v) glucose]. Right panel: Urine samples from 10 nonstabilized individual diabetic patients. GFP fluorescence was measured after 24 hours. Response to glucose was compared with standard urinary dipsticks (lower panels). The lower panels show the glucose reactive band of the urinary dipstick. In the absence of glucose, the band is blue. When glucose is present, the band turns brown. Data from three different experiments performed on different days are depicted by black, gray, and white circles. Each circle corresponds to one replicate (three replicates for each experiment).

(Fig. 4B and note S3) (53–55). First, using the red fluorescent protein (RFP) as a reporter, we tested the response of beads that encapsulated the pCpxP or pYeaR switch to increasing inducer concentrations in

culture medium and observed digital switching detectable with the naked eye (Fig. 4B and fig. S13). The pCpxP switch was activated at a threshold concentration under 0.1 mM glucose, outperforming the

detection limit of urinary dipsticks, the gold standard point-of-care test for glycosuria, by an order of magnitude.

We then tested the beads in urine samples. The pCpxP switch beads produced a robust and specific response in nonpathological urine samples exogenously supplemented with glucose (Fig. 4C, left panel). Finally, we tested the pCpxP switch beads in individual urine samples from 13 patients diagnosed with diabetes but not yet stabilized (Fig. 4C, right panel). The assay reliably detected glycosuria in samples from diabetic patients, with a sensitivity of 88.9% and a specificity of 96.3% (fig. S14). We observed some variability in beads response, which we attributed to our bead fabrication process (see note S3). Improvements in the encapsulation process should increase the reliability of our assay and reduce bead-to-bead variability. Nevertheless, our system was capable of reliably detecting the presence of endogenous glucose in urine from 12 different diabetic patients, suggesting that bactorsensors are relatively robust when faced with interindividual variations in sample composition. Together, our data demonstrate that digital amplifying genetic switches can enable whole-cell biosensor to operate in a clinical assay and detect endogenous biomarkers of disease in patient samples.

DISCUSSION

The past decade has witnessed the development of innovative biodiagnostic technologies and biosensor approaches, promising a new era of fast, versatile, easy-to-use, and reliable point-of-care diagnostic devices (4). However, within the biosensing device family, whole-cell biosensors—despite their potential—have not been able to be translated into real-world clinical applications. Here, we bring whole-cell biosensors closer to medical application by addressing some of the limitations that have hindered their translation to the clinics.

As a prototype, our system demonstrates that digital amplifying switches and logic gates can overcome several typical problems faced in the clinical application of whole-cell biosensors: low signal-to-noise ratios, partial inhibition of the sensor by the samples, and logic processing of multiple biomarkers signals. Digitalizing along with amplifying and multiplexing signal detection improved sensitivity, mediated sharp response profiles, and offered an all-or-none response based on a pathological biomarker threshold (for example, detection of fold change). Moreover, digital switching provided constant outputs and dynamic ranges irrelevant of the control signal and greatly facilitated clinical assay standardization and high-throughput measurements. In addition, transient signals (glucose) that are undetectable in endpoint assays using conventional whole-cell biosensors were detected and stored using our system. This long-term data storage property enables diagnostics tests to be performed and results stored for several months under harsh conditions. Last, we have provided a quantitative framework to evaluate the function and robustness of whole-cell biosensors in clinical samples.

Several hurdles still need to be solved to fully translate whole-cell biosensors into clinical applications. First, methods to engineer new sensing modules tailored to detect ligands of interest are lacking. Current research efforts focus on mining databases for transcriptional regulators that respond to various biological signals and engineering tailored ligand-responsive RNA switches or transmembrane receptors (56–59). Recent encouraging successes suggest that we will witness significant progress in this field in the near future. Multiple sensors that specifically respond to clinically relevant biomarkers could then be

connected to Boolean integrase logic gates to perform multiplexed biomarker detection and analysis in clinical samples (fig. S15).

Second, response times of bactorsensors can be too long for clinical assays. For example, here we measured signal after 18-hour incubations and were able to detect an interpretable output response after 4 to 5 hours (fig. S8). Given the current response time of our assay, it is thus unlikely to compete with test strips for the detection of glycosuria. Further work should thus be devoted to obtaining the shorter response times needed for diagnostic tests, for example, by interfacing our sensors with electronic devices or engineering circuits that rely on post-translational signaling (such as protein phosphorylation). Nevertheless, whereas long measurement times are not compatible with timely diagnosis for certain applications (toxicological emergencies), our system would still be relevant for addressing certain medical questions that require less urgent results such as large-scale population screening, monitoring of chronic disease evolution, or companion diagnostics.

From a broader perspective, our work could be a stepping stone toward future applications that use living cells to perform *in vivo* diagnostics coupled with *in situ* synthesis and delivery of therapeutic molecules (60). Last, although our study addresses robustness and standardization issues essential for commercialization approval, regulatory and safety concerns regarding the use of engineered living organisms in the clinics remain, and societal and ethical questions must be addressed before such agents can be effectively used in the clinic (61). All switches, logic gates, and uses demonstrated or disclosed herein have been contributed to the public domain via the BioBrick public agreement (62).

MATERIALS AND METHODS

Study design

Our goal in this study was to investigate the use of recently developed digital amplifying genetic switches and logic gates (42) to bring the performance of whole-cell biosensor closer to clinical requirements. In particular, we wanted to assess whether digital amplifying switches could overcome typical problems faced in the clinical application of whole-cell biosensors, such as low signal-to-noise ratios, partial inhibition of the sensor by the samples, and logic processing of multiple biomarker signals. Using glycosuria as a model system, we aimed at demonstrating the detection of an endogenous clinically relevant biomarker in a clinical setup using samples from diabetic patients.

We developed a technological platform that was used to build several biosensors capable of detecting various biomolecules. To this aim, we use synthetic biology principles (including standardization and modularity) and provided a method to couple new detection sources to our system. The gates are fully modular (that is, the logic can be easily altered by changing the target DNA sequence for the recombinases) (see figs. S5 and S9).

To evaluate the robustness of our system and its functionality in clinical samples, we used serum and urine pools from healthy individuals as well as urine samples from healthy individuals and diabetic patients. Regarding collection of clinical samples, nonpathological (control) and glycosuric (diabetic) urine samples were obtained from the Department of Endocrinology of the Lapeyronie Hospital, Montpellier, France, under the supervision of E. Renard. Individual informed consents were obtained from the patients and control individuals. Glycosuric urine samples were collected from 10 newly discovered, nonstabilized

diabetic patients. Human serum pools from numerous blood donors were obtained from the Etablissement Français du Sang, Montpellier, France. Serum was heat-inactivated by incubation in a 56°C bath for 30 min. Serum and urine samples were stored at -80°C before use.

Molecular biology

Constructs used in this study were cloned using standard molecular biology procedures or one-step isothermal assembly (63). All enzymes were purchased from New England BioLabs (NEB). PCRs were performed using the Q5 PCR mastermix (NEB, 1-min extension time per kilobase). Most primers were generated using J5 [j5 DNA Assembly Design Automation Software (64); <http://j5.jbei.org>]. Primers were purchased from Eurofins Genomics and IDT (Carlsbad, USA). Detailed information and plasmid maps, primers, and Gblocks sequences can be found in the Supplementary Materials.

Boolean integrase logic

GFP Boolean integrase logic gates and pBAD/pTET plasmid constructs used in this study come from previous work (42). XOR, AND, NOR, and NAND gates were then modified by Gibson assembly to replace GFP with mKate2.

Library design, construction, and screening

To obtain functional synthetic networks, we needed to finely tune gates operation so that translation levels of integrases match relevant clinical dynamic ranges for our application. To introduce diversity within integrase expression cassettes, we built combinatorial libraries of pCpxP and pYeaR promoters driving expression of integrase TP901 and BxB1, by using primers (JB 587, JB588, with G1005) and randomizing (i) RBS (4096 variants), (ii) RBS and initiation codon (8192 variants), and (iii) RBS, initiation codon, and SsrA tag (AXX) (1,179,648 variants). Effective randomization at specific positions was achieved using degenerated primers, and amplified fragments were cloned in a medium copy plasmid (J64100, chloramphenicol resistance). The library was then electroporated in DH10B electrocompetent *E. coli* (Life Technologies) and plated on chloramphenicol plates. After overnight growth, ~8000 colonies per library were counted. The libraries were grown overnight at 30°C in 10 ml of LB with chloramphenicol and mini-prepped. The libraries were then transformed into a chemically competent screening strain containing an episomal XOR-BCD-RFP logic gate. To isolate NO_x-responsive switching clones, the pYeaR library cells were plated, and 600 clones were picked and induced overnight in 400 µl of LB with chloramphenicol with 10 mM NO_x. Clones were then screened using a plate reader by measuring RFP fluorescence levels. Different clones switching after induction were kept for further investigation, yielding controller 1 and controller 2. To obtain controller 3, the TP901 fragment library was cloned in pYeaR_J64100, the library was cotransformed with XOR-RFP gate and induced with 10 mM NO_x, and 400 clones were screened using a plate reader. To isolate glucose-responsive switching clones, the pCpxP-BxB1 library was cotransformed with XOR-RFP gate and sorted using a FACSAria (BD Biosciences): On a first sort step, constitutively switching cells were discarded and the remaining clones were kept and then induced in LB medium containing 0.5% (w/v) glucose for 6 hours. After induction, cells were washed and grown in fresh LB medium overnight at 30°C. On a second sort step, switching cells (~1000 clones) were kept, and nonswitching cells were discarded. One pCpxP-BxB1 controller clone was finally kept for use.

Beads assay

To test the operability of bactorsensors in PVA/alginate beads, beads were inoculated in 300 µl of culture medium with or without inducer, or urine from patient diluted at a ratio of 1:4 in culture medium for a total volume of 300 µl in a 96-well plate. After 24 hours of incubation, fluorescence was read using a synergy H1 plate reader (more details on encapsulation of bacteria in beads can be found in the Supplementary Materials). We concomitantly tested these urines from nonstabilized diabetic patients using the Siemens Multistix 8 SG reagent strip according to the manufacturer's protocol.

Cell culture and data collection

We used *E. coli* DH5αZ1 and *B. subtilis* 168 1A1 for all measurements. Cells were cultivated with shaking at 400 rpm and grown for 18 hours at 25°, 30°, or 37°C, in either Azure Media (Teknova) or LB phosphate buffer adjusted to pH 7. Antibiotics used were carbenicillin (25 µg/ml), kanamycin (30 µg/ml), and chloramphenicol (25 µg/ml) (Sigma). D-Glucose, nitrate, L-ara, and aTc (Sigma) were used at final concentrations of 0.5% (w/v), 0.1 M, 0.5% (w/v), and 200 ng/ml, respectively. Cells were streaked from a glycerol stock, and then one clone was inoculated in 5 ml of LB with carbenicillin and/or chloramphenicol and grown overnight at 30°C. The cells were then diluted at a ratio of 1:200 and grown for 6 hours at 30°C until an optical density (OD) of ~0.5. The cells were then back-diluted at a ratio of 1:100 into 1 ml of azure medium (Teknova) and diluted with urine or serum, induced with 0.5% (w/v) ara, aTc (200 ng/ml), 0.5% (w/v) glucose, or 10 mM NO₃⁻, and grown for 18 hours at 25°C in 96 DeepWell plates. The next morning, the cells were put on ice, and we measured RFP/GFP fluorescence levels (588ex/633em, 485ex/528em, respectively) and OD₆₀₀ using a synergy H1 plate reader (BioTek) and a Beckman Coulter FC 500 flow cytometer recording 50,000 events per samples. Events were gated on forward and side scatter to exclude debris, dead cells, and doublets. The overnight growth, back dilution, and measurement procedure were performed three times on separate days in triplicates. Measurements for each data point were normalized using a reference promoter (BBa_J23101) driving expression of sfGFP (low-copy plasmid pSC101 origin with chloramphenicol resistance).

For functional and genetic memory experiments, cells were cotransformed with pTET/pBAD dual controller plasmid and AND-BCD logic gate plasmid, and induced overnight at 25°C with 0.5% (w/v) ara and aTc (200 ng/ml), in 300 µl of urine, serum, or Azure medium in p96 plates. The plates were kept for 8 months at 4°C. Plasmid DNA was then recovered by scrapping and dissolving the dry cellular residues of cells in phosphate-buffered saline, and extracted using QIAamp (Qiagen) kit. We used specifically designed primers (attL/attR Bxb1 or TP901) to PCR-amplify the recombined targets. For Sanger sequencing experiments, the gate plasmid DNA was amplified using primers G1004 and G1005, and the PCR product was sent for sequencing.

Data analysis and statistics

Experimental values are reported as means ± SD. All experiments were performed at least three times on different days and in triplicate. Data, statistics, graphs, and tables were processed and generated using MATLAB (MathWorks), SigmaPlot (Systat Software Inc.), and the R with ggplot2 package. Flow cytometry was performed using an FC 500 (Beckman Coulter Inc.), and data were analyzed using FlowJo and Flowing Software (Turku Centre for Biotechnology). We used RPU to integrate into clinical measurements an in vivo internal standard for

bactosensor operation and signal generation (45). For signal amplification experiments, amplification was quantified by the gain defined as the 10log ratio between the fractional change in the output signal GFP and the fractional change in the input signal RFP. For receiver operating characteristic analysis, a set of 27 measurements performed in nonpathological urine were compared to 27 measurements performed in urine containing 1% glucose. See the Supplementary Materials for details on calculations.

SUPPLEMENTARY MATERIALS

www.sciencetranslationalmedicine.org/cgi/content/full/7/289/289a83/DC1

Materials and Methods

Notes

Fig. S1. Conceptual workflow for the systematic development of medical bactosensors.

Fig. S2. Bacterial chassis growth characteristics in urine and serum.

Fig. S3. Bacterial chassis viability in urine and serum from single-cell measurements.

Fig. S4. Influence of clinical media (urine and serum) on GFP fluorescence output generation and measurement.

Fig. S5. Population and single-cell measurements of multiplexing Boolean integrase logic gates operation in urine and serum.

Fig. S6. Stability of genetic memory in clinical samples by addressing DNA register with Sanger sequencing.

Fig. S7. Workflow for engineering switches that respond to biological signals over user-defined thresholds.

Fig. S8. Kinetic measurements and transfer functions of promoters and switches.

Fig. S9. Multiplexing detection of glucose and NO_x with AND-BCD-RFP, NAND-BCD-RFP, and NOR-BCD-RFP Boolean integrase logic gates.

Fig. S10. Single-cell measurements of fold changes and DERs for promoters and switches.

Fig. S11. Evaluation of the robustness of inducible systems against clinical media-induced perturbation (urine and serum).

Fig. S12. Comparison of the operational characteristic of AND logic gates with and without the bicistronic device (BCD) for their use in clinical samples.

Fig. S13. Insulation of bactosensors in hydrogel beads and pathological signal detection.

Fig. S14. ROC analysis for bactosensor-mediated detection of glucose in urine.

Fig. S15. Potential modalities of bactosensor-based diagnosis and composability of integrase-based logic for the development of decision-making tests.

Data file S1. Numerical values of OD₆₀₀ and fluorescence from plate reader measurements and calculated RPU's used to develop plots and figures.

Note S1. Experimental design: Use of reference promoters.

Note S2. Genetic design: Use of standardized genetic elements.

Note S3. Bacterial encapsulation toward a clinical format.

References (65–71)

REFERENCES AND NOTES

- D. C. Hay Burgess, J. Wasserman, C. A. Dahl, Global health diagnostics. *Nature* **444**, 1–2 (2006).
- E. Fu, P. Yager, P. N. Floriano, N. Christodoulides, J. T. McDevitt, Perspective on diagnostics for global health. *IEEE Pulse* **2**, 40–50 (2011).
- D. A. Giljohann, C. A. Mirkin, Drivers of biodiagnostic development. *Nature* **462**, 461–464 (2009).
- A. P. F. Turner, Biosensors: Sense and sensibility. *Chem. Soc. Rev.* **42**, 3184–3196 (2013).
- R. De la Rica, M. M. Stevens, Plasmonic ELISA for the ultrasensitive detection of disease biomarkers with the naked eye. *Nat. Nanotechnol.* **7**, 821–824 (2012).
- X. Chi, D. Huang, Z. Zhao, Z. Zhou, Z. Yin, J. Gao, Nanoprobes for in vitro diagnostics of cancer and infectious diseases. *Biomaterials* **33**, 189–206 (2012).
- A. W. Martinez, S. T. Phillips, G. M. Whitesides, E. Carrilho, Diagnostics for the developing world: Microfluidic paper-based analytical devices. *Anal. Chem.* **82**, 3–10 (2010).
- P. Yager, T. Edwards, E. Fu, K. Helton, K. Nelson, M. R. Tam, B. H. Weigl, Microfluidic diagnostic technologies for global public health. *Nature* **442**, 412–418 (2006).
- M. U. Ahmed, I. Saem, P. C. Wu, A. S. Brown, Personalized diagnostics and biosensors: A review of the biology and technology needed for personalized medicine. *Crit. Rev. Biotechnol.* **34**, 180–196 (2014).
- V. Gubala, L. F. Harris, A. J. Ricco, M. X. Tan, D. E. Williams, Point of care diagnostics: Status and future. *Anal. Chem.* **84**, 487–515 (2012).
- L. Su, W. Jia, C. Hou, Y. Lei, Microbial biosensors: A review. *Biosens. Bioelectron.* **26**, 1788–1799 (2011).
- J. R. Van der Meer, S. Belkin, Where microbiology meets microengineering: Design and applications of reporter bacteria. *Nat. Rev. Microbiol.* **8**, 511–522 (2010).
- N. Raut, G. O'Connor, P. Pasini, S. Daunert, Engineered cells as biosensing systems in biomedical analysis. *Anal. Bioanal. Chem.* **402**, 3147–3159 (2012).
- American Society for Microbiology, *Manual of Industrial Microbiology and Biotechnology* (ASM Press, Washington, DC, 2010).
- A. Date, P. Pasini, A. Sangal, S. Daunert, Packaging sensing cells in spores for long-term preservation of sensors: A tool for biomedical and environmental analysis. *Anal. Chem.* **82**, 6098–6103 (2010).
- F. Cortés-Salazar, S. Beggah, J. R. van der Meer, H. H. Girault, Electrochemical As(III) whole-cell based biochip sensor. *Biosens. Bioelectron.* **47**, 237–242 (2013).
- A. Prindle, P. Samayoa, I. Razinkov, T. Danino, L. S. Tsimring, J. Hasty, A sensing array of radically coupled genetic 'biopixels'. *Nature* **481**, 39–44 (2011).
- S. Melamed, T. Elad, S. Belkin, Microbial sensor cell arrays. *Curr. Opin. Biotechnol.* **23**, 2–8 (2012).
- J. Horswell, S. Dickson, Use of biosensors to screen urine samples for potentially toxic chemicals. *J. Anal. Toxicol.* **27**, 372–376 (2003).
- C. Lewis, S. Beggah, C. Pook, C. Guitart, C. Redshaw, J. R. van der Meer, J. W. Readman, T. Galloway, Novel use of a whole cell *E. coli* bioreporter as a urinary exposure biomarker. *Environ. Sci. Technol.* **43**, 423–428 (2009).
- A. Roda, P. Pasini, N. Mirasoli, M. Guardigli, C. Russo, M. Musiani, M. Baraldini, Sensitive determination of urinary mercury (II) by a bioluminescent transgenic bacteria-based biosensor. *Anal. Lett.* **34**, 29–41 (2001).
- K. Turner, S. Xu, P. Pasini, S. Deo, L. Bachas, S. Daunert, Hydroxylated polychlorinated biphenyl detection based on a genetically engineered bioluminescent whole-cell sensing system. *Anal. Chem.* **79**, 5740–5745 (2007).
- E. Michelini, M. Magliulo, P. Leskinen, M. Virta, M. Karp, A. Roda, Recombinant cell-based bioluminescence assay for androgen bioactivity determination in clinical samples. *Clin. Chem.* **51**, 1995–1998 (2005).
- H. M. Alloush, E. Anderson, A. D. Martin, M. W. Ruddock, J. E. Angell, P. J. Hill, P. Mehta, M. A. Smith, J. G. Smith, V. C. Salisbury, A bioluminescent microbial biosensor for in vitro pretreatment assessment of cytarabine efficacy in leukemia. *Clin. Chem.* **56**, 1862–1870 (2010).
- D. Endy, Foundations for engineering biology. *Nature* **438**, 449–453 (2005).
- C. J. Paddon, J. D. Keasling, Semi-synthetic artemisinin: A model for the use of synthetic biology in pharmaceutical development. *Nat. Rev. Microbiol.* **12**, 355–367 (2014).
- M. N. Thaker, W. Wang, P. Spanogiannopoulos, N. Waglechner, A. M. King, R. Medina, G. D. Wright, Identifying producers of antibacterial compounds by screening for antibiotic resistance. *Nat. Biotechnol.* **31**, 922–927 (2013).
- P. K. Ajikumar, W. H. Xiao, K. E. Tyo, Y. Wang, F. Simeon, E. Leonard, O. Mucha, T. H. Phon, B. Pfeifer, G. Stephanopoulos, Isoprenoid pathway optimization for Taxol precursor overproduction in *Escherichia coli*. *Science* **330**, 70–74 (2010).
- K. Thodey, S. Galanie, C. D. Smolke, A microbial biomanufacturing platform for natural and semisynthetic opioids. *Nat. Chem. Biol.* **10**, 837–844 (2014).
- W. C. Ruder, T. Lu, J. J. Collins, Synthetic biology moving into the clinic. *Science* **333**, 1248–1252 (2011).
- W. Weber, M. Fussenegger, Emerging biomedical applications of synthetic biology. *Nat. Rev. Genet.* **13**, 21–35 (2011).
- A. G. Planson, P. Carbonell, I. Grigoras, J. L. Faulon, A retrosynthetic biology approach to therapeutics: From conception to delivery. *Curr. Opin. Biotechnol.* **6**, 948–956 (2012).
- Z. Xie, L. Wroblewska, L. Prochazka, R. Weiss, Y. Benenson, Multi-input RNAi-based logic circuit for identification of specific cancer cells. *Science* **333**, 1307–1311 (2011).
- S. Culler, K. G. Hoff, C. D. Smolke, Reprogramming cellular behavior with RNA controllers responsive to endogenous proteins. *Science* **330**, 1251–1255 (2010).
- C. Kemmer, M. Gitzinger, M. Daoud-El Baba, V. Djonov, J. Stelling, M. Fussenegger, Self-sufficient control of urate homeostasis in mice by a synthetic circuit. *Nat. Biotechnol.* **28**, 355–360 (2010).
- F. Duan, K. L. Curtis, J. C. March, Secretion of insulinotropic proteins by commensal bacteria: Rewiring the gut to treat diabetes. *Appl. Environ. Microbiol.* **23**, 7437–7438 (2008).
- Y. Y. Chen, M. C. Jensen, C. D. Smolke, Genetic control of mammalian T-cell proliferation with synthetic RNA regulatory systems. *Proc. Natl. Acad. Sci. U.S.A.* **107**, 8531–8536 (2010).
- T. K. Lu, J. Bowers, M. S. Koeis, Advancing bacteriophage-based microbial diagnostics with synthetic biology. *Trends Biotechnol.* **31**, 325–327 (2013).
- D. Ausländer, B. Eggerschwiler, C. Kemmer, B. Geering, S. Ausländer, M. Fussenegger, A designer cell-based histamine-specific human allergy profiler. *Nat. Commun.* **5**, 4408 (2014).
- Y. Benenson, Biomolecular computing systems: Principles, progress and potential. *Nat. Rev. Genet.* **7**, 455–468 (2012).
- J. A. Brophy, C. A. Voigt, Principles of genetic circuit design. *Nat. Methods* **5**, 508–520 (2014).

42. J. Bonnet, P. Yin, M. E. Ortiz, P. Subsoontorn, D. Endy, Amplifying genetic logic gates. *Science* **340**, 599–603 (2013).
43. V. K. Mutalik, J. C. Guimaraes, G. Cambray, C. Lam, M. J. Christoffersen, Q. A. Mai, A. B. Tran, M. Paull, J. D. Keasling, A. P. Arkin, D. Endy, Precise and reliable gene expression via standard transcription and translation initiation elements. *Nat. Methods* **10**, 354–360 (2013).
44. C. Lou, B. Stanton, Y. J. Chen, B. Munsky, C. A. Voigt, Ribozyme-based insulator parts buffer synthetic circuits from genetic context. *Nat. Biotechnol.* **30**, 1137–1142 (2012).
45. J. R. Kelly, A. J. Rubin, J. H. Davis, C. M. Ajo-Franklin, J. Cumbers, M. J. Czar, K. de Mora, A. L. Glielberman, D. D. Monie, D. Endy, Measuring the activity of BioBrick promoters using an in vivo reference standard. *J. Biol. Eng.* **3**, 4 (2009).
46. J. Bonnet, P. Subsoontorn, D. Endy, Rewritable digital data storage in live cells via engineered control of recombination directionality. *Proc. Natl. Acad. Sci. U.S.A.* **109**, 8884–8889 (2012).
47. J. N. Sharma, A. Al-Omran, S. S. Parvathy, Role of nitric oxide in inflammatory diseases. *Inflammopharmacology* **15**, 252–259 (2007).
48. H. Y. Lin, P. J. Bledsoe, V. Stewart, Activation of *yeaR-yoaG* operon transcription by the nitrate-responsive regulator NarL is independent of oxygen-responsive regulator Fnr in *Escherichia coli* K-12. *J. Bacteriol.* **189**, 7539–7548 (2007).
49. C. M. Farrell, A. D. Grossman, R. T. Sauer, Cytoplasmic degradation of *ssrA*-tagged proteins. *Mol. Microbiol.* **57**, 1750–1761 (2005).
50. American Diabetes Association, Standards of medical care in diabetes—2014. *Diabetes Care* **37**, S14–S80 (2014).
51. B. P. Lima, H. Antelmann, K. Gronau, B. K. Chi, D. Becher, S. R. Brinsmade, A. J. Wolfe, Involvement of protein acetylation in glucose-induced transcription of a stress-responsive promoter. *Mol. Microbiol.* **81**, 1190–1204 (2011).
52. A. J. Wolfe, N. Parikh, B. P. Lima, B. Zemaitaitis, Signal integration by the two component signal transduction response regulator CpxR. *J. Bacteriol.* **190**, 2314–2322 (2008).
53. P. S. J. Cheetham, K. W. Blunt, C. Bocke, Physical studies on cell immobilization using calcium alginate gels. *Biotechnol. Bioeng.* **21**, 2155–2168 (1979).
54. Team: Paris Bettencourt—2012.igem.org. (2012); http://2012.igem.org/Team:Paris_Bettencourt.
55. T. Takei, K. Ikeda, H. Ijima, K. Kawakami, Fabrication of poly(vinyl alcohol) hydrogel beads crosslinked using sodium sulfate for microorganism immobilization. *Process Biochem.* **46**, 566–571 (2011).
56. H. Salis, A. Tamsir, C. A. Voigt, Engineering bacterial signals and sensors. *Contrib. Microbiol.* **16**, 194–225 (2009).
57. M. N. Win, J. C. Liang, C. D. Smolke, Frameworks for programming biological function through RNA parts and devices. *Chem. Biol.* **16**, 298–310 (2009).
58. W. A. Lim, Designing customized cell signalling circuits. *Nat. Rev. Mol. Cell Biol.* **11**, 393–403 (2010).
59. M. Sadelain, R. Brentjens, I. Rivière, The promise and potential pitfalls of chimeric antigen receptors. *Curr. Opin. Immunol.* **21**, 215–223 (2009).
60. J. W. Kotula, S. J. Kerns, L. A. Shaket, L. Siraj, J. J. Collins, J. C. Way, P. A. Silver, Programmable bacteria detect and record an environmental signal in the mammalian gut. *Proc. Natl. Acad. Sci. U.S.A.* **111**, 4838–4843 (2014).
61. P. B. Archana Chugh, Synthetic biology based biosensors and the emerging governance issues. *Curr. Synth. Syst. Biol.* **1**, 108 (2013).
62. BioBrick public agreement, <https://biobricks.org/bpa>
63. D. G. Gibson, L. Young, R. Y. Chuang, J. C. Venter, C. A. Hutchison III, H. O. Smith, Enzymatic assembly of DNA molecules up to several hundred kilobases. *Nat. Methods* **6**, 343–345 (2009).
64. N. J. Hillson, R. D. Rosengarten, J. D. Keasling, j5 DNA assembly design automation software. *ACS Synth. Biol.* **1**, 14–21 (2012).
65. R. Kwok, Five hard truths for synthetic biology. *Nature* **463**, 288–290 (2010).
66. L. J. Bugaj, D. V. Schaffer, Bringing next-generation therapeutics to the clinic through synthetic biology. *Curr. Opin. Chem. Biol.* **16**, 355–361 (2012).
67. A. P. Arkin, A wise consistency: Engineering biology for conformity, reliability, predictability. *Curr. Opin. Chem. Biol.* **17**, 893–901 (2013).
68. A. Struss, P. Pasini, C. M. Ensor, N. Raut, S. Daunert, Paper strip whole cell biosensors: A portable test for the semiquantitative detection of bacterial quorum signaling molecules. *Anal. Chem.* **82**, 4457–4463 (2010).
69. E. Michelini, A. Roda, Staying alive: New perspectives on cell immobilization for biosensing purposes. *Anal. Bioanal. Chem.* **402**, 1785–1797 (2012).
70. J. Lehtinen, J. Nuutila, E. M. Lilius, Green fluorescent protein–propidium iodide (GFP-PI) based assay for flow cytometric measurement of bacterial viability. *Cytometry A* **60**, 165–172 (2004).
71. K. Otto, T. J. Silhavy, Surface sensing and adhesion of *Escherichia coli* controlled by the Cpx-signaling pathway. *Proc. Natl. Acad. Sci. U.S.A.* **99**, 2287–2292 (2002).

Acknowledgments: We thank P. Amar, N. Salvétat, and members of the Endy Lab for fruitful discussions; C. Duperray and N. Vié from the Montpellier Rio Imaging cytometry platform and C. Crumpton and M. Bigos from the Stanford Shared FACS Facility for the cytometry experiments; the Centre Regional d'Imagerie Cellulaire platform and C. Cazeville for scanning electron microscopy experiments; the Paris Bettencourt iGEM team 2012 for igniting our interest in the encapsulation of bacteria into alginate beads; and the patients for participating in this study. **Funding:** This work was supported by Stanford University, the France-Stanford Center for Interdisciplinary Studies, the Institut National de la Santé et de la Recherche Médicale (INSERM), and the Centre National pour la Recherche Scientifique (CNRS). A.C. is a recipient of a fellowship from the French Ministry of Health and a pharmacy resident at the Montpellier Centre Hospitalier Régional Universitaire (CHRU). J.B. is supported by grants from the INSERM Avenir-ATIP program and the Bettencourt Schuller Foundation. **Author contributions:** A.C., J.B., D.E., and F.M. designed the study. A.C. and J.B. performed library construction and screening. A.C. performed all other experiments and the statistical analysis. E.R. collected clinical samples. A.C. and J.B. analyzed and displayed the data and wrote the manuscript. All authors participated in the interpretation of the results and in the editing of the manuscript. **Competing interests:** The authors declare that they have no competing financial interests. **Data and materials availability:** Sequences for constructs generated in this study are deposited in GenBank (accession numbers: KM234313-23 and KM347896). Plasmids are available from Addgene.

Submitted 24 November 2014

Accepted 21 April 2015

Published 27 May 2015

10.1126/scitranslmed.aaa3601

Citation: A. Courbet, D. Endy, E. Renard, F. Molina, J. Bonnet, Detection of pathological biomarkers in human clinical samples via amplifying genetic switches and logic gates. *Sci. Transl. Med.* **7**, 289ra83 (2015).

Editor's Summary

A little help from our (little) friends

It's only logical: Translation of diagnostics to home health care or remote settings requires simple methods for measuring markers in complex clinical samples. And living cells—with their ability to detect biomolecules, process the signal, and respond—are logical choices as biosensing devices. The recent buzz on the human microbiota has expanded our view of bacteria beyond infectious enemies to metabolic buddies. Now, Courbet *et al.* refine that view further by engineering bacteria to serve as whole-cell diagnostic biosensors in human biological samples.

Although whole-cell biosensors have been shown to serve as analytical tools, their quirky operation and low signal-to-noise ratio in complex clinical samples have limited their use as diagnostic devices in the clinic. The authors engineered bacterial biosensors capable of signal digitization and amplification, multiplexed signal processing (with the use of Boolean logic gates), and months-long data storage. As a proof of concept, the "bactosensors" detected pathological levels of glucose in urine from diabetic patients, providing a framework for the design of sensor modules that detect diverse biomarkers for diagnostics.

A complete electronic version of this article and other services, including high-resolution figures, can be found at:

<http://stm.sciencemag.org/content/7/289/289ra83.full.html>

Supplementary Material can be found in the online version of this article at:

<http://stm.sciencemag.org/content/suppl/2015/05/22/7.289.289ra83.DC1.html>

Related Resources for this article can be found online at:

<http://stm.sciencemag.org/content/scitransmed/5/179/179ps7.full.html>

<http://stm.sciencemag.org/content/scitransmed/6/267/267ra174.full.html>

<http://stm.sciencemag.org/content/scitransmed/7/283/283rv3.full.html>

<http://stm.sciencemag.org/content/scitransmed/6/253/253rv2.full.html>

<http://stm.sciencemag.org/content/scitransmed/7/273/273re1.full.html>

Information about obtaining **reprints** of this article or about obtaining **permission to reproduce this article** in whole or in part can be found at:

<http://www.sciencemag.org/about/permissions.dtl>